Performance Characteristics of Distinct Lightning Detection Networks Covering Belgium

DIETER R. POELMAN

Royal Meteorological Institute of Belgium, Brussels, Belgium

WOLFGANG SCHULZ

OVE-ALDIS, Vienna, Austria

CHRISTIAN VERGEINER

Institute of High Voltage Engineering and System Management, Graz University of Technology, Graz, Austria

ABSTRACT

This study reports results from electric field measurements coupled to high-speed camera observations of cloud-to-ground lightning to test the performance of lightning location networks in terms of its detection efficiency and location accuracy. The measurements were carried out in August 2011 in Belgium, during which 57 negative cloud-to-ground flashes, with a total of 210 strokes, were recorded. One of these flashes was followed by a continuing current of over 1 s—one of the longest ever observed in natural negative cloud-to-ground lightning. Lightning data gathered from the lightning detection network operated by the Royal Meteorological Institute of Belgium [consisting of a network employing solely Surveillance et Alerte Foudre par Interférométrie Radioélectrique (SAFIR) sensors and a network combining SAFIR and LS sensors], the European Cooperation for Lightning Detection (EUCLID), Vaisala's Global Lightning Detection network GLD360, and the Met Office's long-range Arrival Time Difference network (ATDnet) are evaluated against this ground-truth dataset. It is found that all networks are capable of detecting over 90% of the observed flashes, but a larger spread is observed at the level of the individual strokes. The median location accuracy varies between 0.6 and 1 km, except for the SAFIR network, locating the ground contacts with 6.1-km median accuracy. The same holds for the reported peak currents, where a good correlation is found among the networks that provide peak current estimates, apart from the SAFIR network being off by a factor of 3.

1. Introduction

Lightning location systems (LLSs) have been used for more than 20 years and employ different types of sensors operating at very low/low frequencies (VLFs/LFs) up to very high frequencies (VHFs), enabling the user to detect cloud-to-ground (CG) lightning and/or intracloud (IC) electrical activity. Depending on the available sensor information, either direction finding, a time-of-arrival (TOA) technique, or a combination of them can be used to process the raw sensor data into valid locations.

Various methods can be applied to investigate the performance of a lightning location network. For instance, lightning detections could be linked to outage reports of high-voltage transmission lines or damage/insurance claims (e.g., Diendorfer and Schulz 2003). In addition, data from different LLSs can be intercompared when having an overlapping region in common (e.g., Poelman 2011). However, the most straightforward way to determine the performance of an LLS is through the use of ground-truth data. Such data can be gathered by means of observations of lightning to towers (e.g., Diendorfer 2010), measurements of rocket-triggered lightning (e.g., Jerauld et al. 2005; Nag et al. 2011), or via video and electric field (E-field) measurements (e.g., Idone et al. 1998a,b; Schulz et al. 2010). However, contrary to intercomparison studies typically covering larger areas

Corresponding author address: Dieter R. Poelman, Royal Meteorological Institute of Belgium, Ringlaan 3, 1180 Brussels, Belgium.
E-mail: dieter.poelman@meteo.be

and time span, are ground-truth campaigns solely valid for a specific time and location. In addition, there are differences between tower/triggered and video/E-field measurements. For instance, observations of lightning to towers are restricted to the tower position, unlike E-field and video measurements. Thus, results coming from tower data are solely valid for the position of the tower. In addition, observations of tower and triggered lightning give the location accuracy (LA) directly and also show a potential systematic error. E-field and video measurements in turn provide solely an upper limit to the LA, as one cannot be undoubtedly sure whether the channel has the same ground striking point for all the strokes in a flash (Biagi et al. 2007). Note that with the latter method, a potential systematic location error in the data cannot be retrieved by looking at the spatial differences between the individual strokes, since the exact location of the discharge is impossible to be determined with a single camera in an open field, neither in combination with an E-field instrument. Contrary to lightning to towers and triggered lightning, video and E-field studies provide detection efficiency (DE) estimates for first strokes, in addition to the subsequent stroke DE. After all, first strokes in tower/triggered lightning cannot be compared to first strokes in natural lightning.

In this paper, we present for the first time results of the performance in terms of detection efficiency and location accuracy of five different lightning detection networks covering Belgium, based on a ground-truth campaign during August 2011 using E-field and high-speed camera observations. In addition, estimated peak currents among the networks are examined, as well as the positions of corresponding strokes relative to each other. In section 2 the measurement setup is described together with the collected data. The networks for which we determine the performance are presented in section 3. We report on the resulting performance characteristics in section 4 and summarize in section 5.

2. Measurements and data

A GPS-synchronized E-field measurement (FM) system is used, consisting of a flat plate electric field antenna, an integrator, a fiber optics link, and a high-speed camera. In this way, the change of the electric field during lightning activity up to a few tens of kilometers away is recorded continuously. The camera records 200 frames per second, enough to separate the individual strokes that exist in a multistroke flash. For more details on the operational and technical aspects of the FM system, we refer the interested reader to Schulz et al. (2005) and Schulz and Saba (2009).
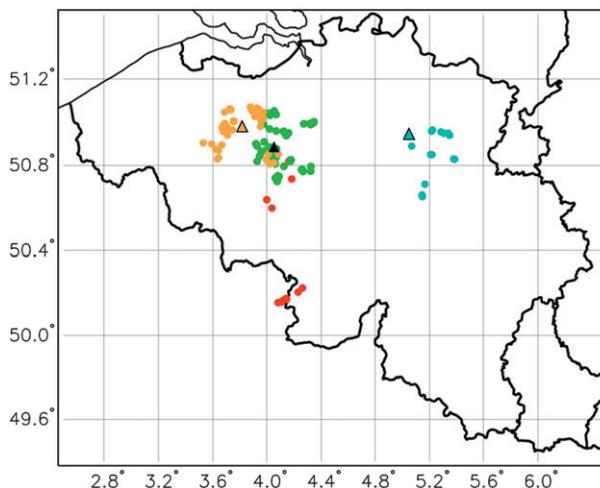

FIG. 1. The positions of the observed strokes are indicated (dots) and color coded by day (22 Aug: red and blue, 23 Aug: green, 26 Aug: orange). The different camera positions are plotted as well (triangles) with a color corresponding to the stroke colors. However, the red and green strokes share a common camera position (solid black).

The measurements were carried out during August 2011 in Belgium. Even though a favorable period to encounter electrical activity, storm cells were observed to overpass Belgium only on 18, 22, 23, and 26 August. However, only data from 22 August (2000–2300 UTC), 23 August (0700–0800 UTC), and 26 August (0430–0530 UTC) are found to be of sufficient quality for further investigation. In the dataset we find 57 negative flashes with a total of 210 strokes that are accepted for additional analysis. Note that the strokes detected by the different networks are grouped into flashes in a same manner to yield compatible flash data as follows. An individual stroke belongs to a particular flash if the time difference between the first recorded stroke of the flash and the stroke in question is less than 1 s and the spatial difference is less than 10 km. In addition an interstroke criterion $\Delta t < 0.5$ s is applied as well. Note that the only flashes used are those we have complete knowledge of all the occurred strokes. This means that we discard flashes that do not have a clear lightning channel to ground in the video and the related E-field cannot be clearly identified as coming from the CG flash. The ground terminations of the different return strokes (RSs) as located by the European Cooperation for Lightning Detection (EUCLID) as well as the different camera positions are plotted in Fig. 1.

In what follows, we evaluate solely the performance of the networks against negative CGs, since not enough data are collected to make valuable statistics for positive CGs.
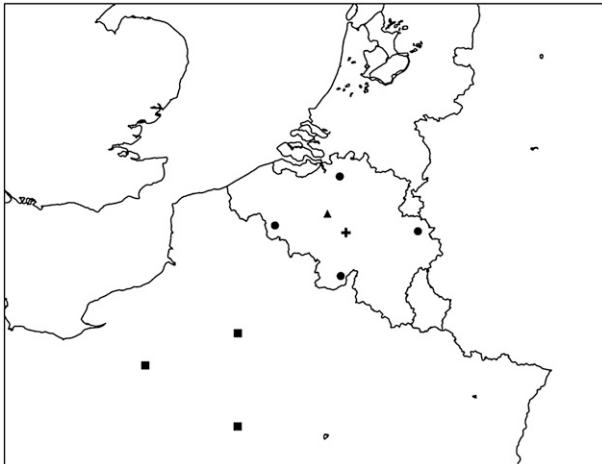
FIG. 2. In addition to the four SAFIR sensors of OP (dots), TP uses data from an extra, fifth, SAFIR sensor (triangle), an LS7001 (cross), and three LS8000 sensors (squares) at the time of the campaign.

3. Networks

a. Belgian lightning detection network

The Royal Meteorological Institute of Belgium (RMI) has been operating a LLS since 1992. This network consists of four Surveillance et Alerte Foudre par Interférométrie Radioélectrique[1] (SAFIR) sensors in Dourbes, Oelegem, La Gileppe, and Mourcourt; see Fig. 2. Within the current operational processor (OP), the localization of lightning discharges is operated in the VHF band and uses solely the latter four sensors. An interferometric lightning location retrieval method for VHF signals is used to retrieve after triangulation the location of the sources. In addition, the sensors are equipped with an E-field antenna detecting the LF RS signature, allowing the discrimination between IC and CG electrical signals. Once an LF signal is detected, the CG stroke is given the location of a time-correlated VHF signal.

Besides OP, RMI is running in parallel Vaisala's Total Lightning Processor (TLP) as a processor in test phase (TP). TP uses a combination of TOA and magnetic direction finding (MDF) to locate CG discharges. Note that not only does the method differ for locating CGs between OP and TP but also the amount of sensors that can contribute to a valid solution. Besides the former four SAFIR sensors used by OP, TP receives raw data from an extra, fifth, SAFIR sensor positioned in Ukkel. In addition, at the time of the campaign, TP shared data with Vaisala's demonstration network around Paris, France, in cooperation with Météorage. This nonoperational network provides TP with lightning data from three LS8000 sensors in Évreux, Compiègne, and Renardières. An extra LS7001 is placed in Ernage, Belgium, for study purposes, but it was only operational from 26 August onward, bringing the total available sensors to nine for TP.

b. EUCLID

In 2001 several countries, that is, Austria, France, Germany, Italy, Norway, and Slovenia, started EUCLID, with the goal to provide Europe-wide lightning data with nearly homogeneous quality. Subsequently, Spain, Portugal, Finland, and Sweden joined EUCLID as well. EUCLID is special, in the sense that the individual partners are highly motivated to run their individual networks with state-of-the-art lightning sensors. As of August 2011 the EUCLID network employs 142 sensors, see Fig. 3, of which there are 4 Lightning Positioning and Tracking System (LPATS)[2] III, 13 LPATS IV, 1 SAFIR, 16 Improved Performance from Combined Technology (IMPACT)[3], 42 IMPACT Enhanced Sensitivity and Performance (ES/ESP), and 66 LS7000[4] sensors (oldest to newest), all operating over the same frequency range with individually calibrated gains and sensitivities. Data from all these sensors are processed in real-time using a single common central processor, which also produces daily performance analysis for each of the sensors. This ensures that the resulting data are as consistent as possible throughout Europe. In fact, the Europe-wide data produced by EUCLID are frequently of higher quality than the data produced by individual country networks due to the implicit redundancy produced by shared sensor information.

c. GLD360

Vaisala's new global lightning detection network, named GLD360, was developed in collaboration with Stanford University and has been operational since the beginning of 2010. It employs a set of sensors with orthogonal magnetic loop antennas operating at VLFs that estimate an arrival azimuth for each measured sferic. A method is then applied that cross correlates the arriving

---

[1] The sensor combines a localization antenna operating at VHF (110–118 MHz) and a discrimination antenna at LF (300–3 MHz).

[2] LPATS sensors are LF wideband (1–350 kHz) receivers, using TOA for position retrieval.

[3] IMPACT sensors combine MDF and TOA techniques to determine the location of CGs.

[4] The operating frequency for a sensor of type LS700x is 400 Hz to 400 kHz (VLF/LF). The sensor is optimized for detecting CG return strokes and large-amplitude cloud pulses combining MDF and TOA technology.
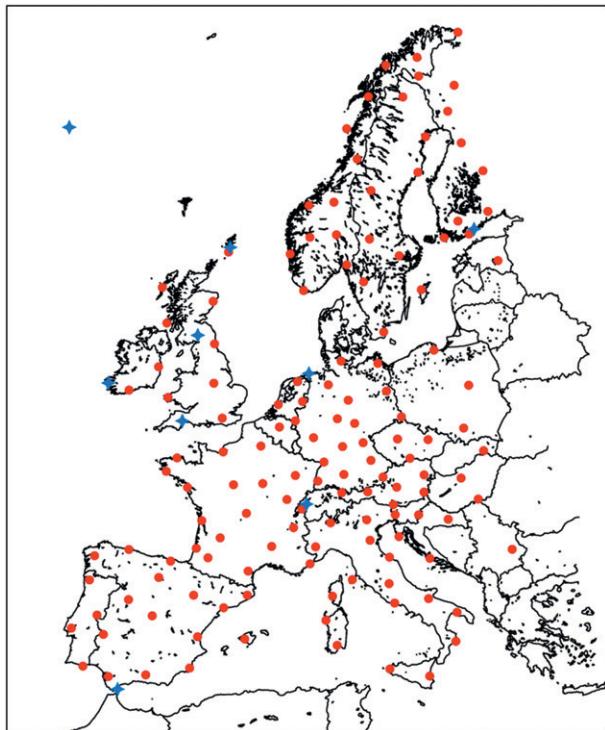
FIG. 3. The locations of the sensors employed by EUCLID (dots, red) and the positions of some of the ATDnet sensors (stars, blue) are indicated.

FIG. 4. Histogram of the 153 interstroke intervals in 57 flashes.

sferic waveform from individual strokes to a so-called waveform bank, containing a catalogue of expected empirical waveforms seen by the sensor. The best match estimates the propagation distance and identifies a reliable arrival time estimate. Subsequently, propagation corrections by the central processor are applied to each arrival time measurement. Finally, the position and time of the lightning discharge are found by minimizing a cost function defined by the arrival time and azimuth errors of the sensors. In addition, GLD360 provides the polarity and peak current estimates. A more thorough description of the network is found in Said et al. (2010, 2011).

d. ATDnet

The Met Office (UKMO) owns and operates a long-range lightning location network called the Arrival Time Difference network (ATDnet; Lee 1986, 1989). The network has been in continuous operation since its initiation in 1987 and has undergone significant expansion and development in recent years, with the network currently consisting of 18 sensors deployed across Europe and Asia; however, only 11 of the sensors are currently used for operational processing, giving good coverage over all of Europe. The seven additional sensors are
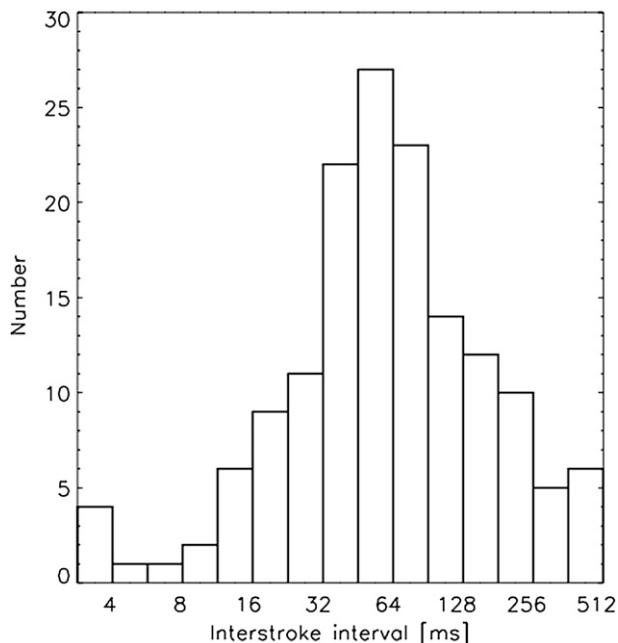
positioned farther afield and are intended to provide improved long-range coverage in the future. The network exploits VLF radio pulses emitted by lightning RSs, locating the source by the accurate timing of arrival when the peak energy of the emitted waveform arrives at each sensor site. As VLF signals propagate over thousands of kilometers with low attenuation, ATDnet can locate lightning over 10 000 km from the network center in northwest Europe. The positions of the operational sensors in Europe are plotted in Fig. 3.

4. Analysis

The final dataset includes 57 flashes, containing a total of 210 strokes. From this a mean multiplicity of 3.7 strokes per flash is found, with a standard deviation of 1.4. Similar multiplicities are found in comparable studies (e.g., Schulz et al. 2010; Saba et al. 2006; Rakov and Uman 1990a). The distribution of all 153 interstroke intervals is plotted in Fig. 4. We deduce a mean and median time interval between successive RSs of 0.096 and 0.058 s, respectively, with a minimum of 872×10^{-6} s and a maximum of 0.46 s. The mean standard deviation is 3.23×10^{-4} s. This distribution is similar to what is found in the literature for negative CG strokes (e.g., Rakov and Uman 1990a).

Besides the scope of this paper, it is worth mentioning that one flash has been observed with a continuing current (CC) of more than 1 s. Although the image quality is not conclusive to determine the exact length of the
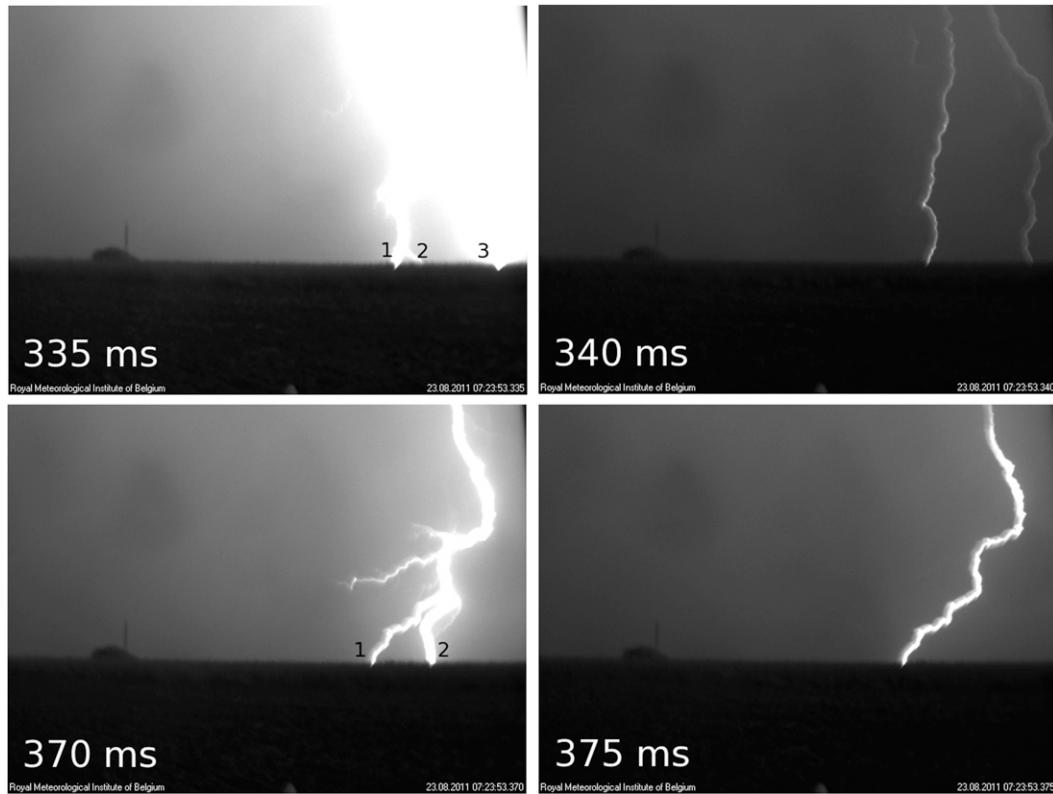
FIG. 5. Frame sequence of the flash with a CC exceeding 1 s. Notice the multiple ground contacts of the two strokes in the images indicated in frames 335 and 370 ms. The long CC was observed after the second RS in frame 370 ms, that is, channel "1."

observed CC, the channel persists to light up until 1.016 s after the RS. Clearly exceeding 40 ms, this CC can be classified as a long CC following Kitagawa et al. (1962) and Brook et al. (1962), and to our knowledge it is one of the longest CCs ever observed of natural negative CG lightning. The long CC was observed at the end of the flash, following the second RS, with an interstroke interval of 34 ms. Note that the first stroke had three and the second stroke had two different ground contact points, as seen in Fig. 5. Each of the RSs has been observed by only one LLS, obtaining a modest negative peak current of −5.7 kA for the first RS (as measured by EUCLID) and −5.1 kA for the second RS (as measured by GLD360). The characteristics of the long CC are in accordance with the results presented in Rakov and Uman (1990a, 1991) and Saba et al. (2006): 1) long CCs are initiated by subsequent strokes within a multistroke flash, 2) strokes initiating long CCs are usually preceded by relatively short interstroke intervals, and 3) strokes initiating long CCs tend to exhibit relatively small peak currents.

Table 1 lists the DE, LA, and median peak current (I_p) for the detected strokes and flashes for each network. Values for the 95% confidence interval are given in

parentheses for LA and I_p. A flash/stroke DE is found of 93/70%, 92/64%, 100/84%, 96/70%, and 88/58% for OP, TP, EUCLID, GLD360, and ATDnet, respectively. The DEs in this study for EUCLID are in line with previous studies, reporting a flash DE of 98% and stroke DEs ranging between 83% and 84% (Schulz 2011). The latter results are based on a sample of 154 flashes and 542 strokes, spread over two ground-truth campaigns in 2010 and 2011 in Austria. The DEs found in this study for GLD360 exceed the expected value for the CG flash DE of 70% by far, as proclaimed by Vaisala. Other studies validating GLD360 against the U.S. National Lightning Detection Network (NLDN) show CG flash DEs ranging between 86% and 92% (Demetriades et al. 2010) or against the Brazilian Lightning Detection Network (BrasilDAT) of about 16% (Naccarato et al. 2010). In the case of ATDnet, the projected stroke DE of ~90% calculated over Europe (Keogh et al. 2006) is higher than the 58% in the present analysis, but of the same order when cross correlated to the Austrian Lightning Detection and Information System (ALDIS; Gaffard et al. 2008). Note that when analyzing the day-to-day DE of ATDnet, a large deviation is observed between

TABLE 1. DE, LA, and I_p for the individual networks. In addition, 95% confidence intervals are reported in parentheses.

	Stroke DE (%)	First stroke DE (%)	Subsequent stroke DE (%)	Flash DE (%)	Median LA (km)	No. of strokes*	Median stroke I_p (kA)	Median first stroke I_p (kA)	Median subsequent stroke I_p (kA)
OP	70	84	64	93	6.1 (0, 8.8)	13	−55.2 (−64, −47)	−70.1 (−96, −52)	−47.6 (−59, −41)
TP	64	88	56	92	1.0 (0.7, 3.6)	12	−19.0 (−21, −16)	−22.5 (−33, −15)	−19.0 (−21, −15)
EUCLID	84	98	79	100	0.6 (0.2, 1.9)	23	−18.2 (−21, −16)	−23.4 (−32, −17)	−17.4 (−20, −14)
GLD360	70	79	66	96	0.9 (0.5, 3.3)	22	−18.3 (−21, −15)	−24.1 (−40, −15)	−15.8 (−20, −13)
ATDnet	58	75	51	88	1.0 (0.6, 2)	13	—	—	—

* The amount of strokes used to estimated the LA.

the DE on 22 August (23%, 2000–2300 UTC), 23 August (60%, 0700–0800 UTC), and 26 August (75%, 0430–0530 UTC). Hence, the averaged stroke DE of 58% over the three days for ATDnet is heavily influenced by the low DE on 22 August at night. On the other hand, GLD360, being a long-range LLS as well, does not seem to experience a similar diurnal variation with DEs of 79%, 71%, and 61% on 22, 23, and 26 August, respectively. It seems therefore that ATDnet's performance is more influenced by the diurnal cycle compared to GLD360.

When distinguishing the detection capabilities between first and subsequent strokes, it is found that the first stroke has a greater chance to be detected than the subsequent strokes for all the networks. This is not surprising, as in general the first stroke in a flash exhibits a higher peak current compared to the subsequent strokes in negative CG flashes; see Table 1.

To determine the LA, only strokes that follow the same stroke channel as determined from the images are used. As such, these strokes are assumed to strike ground at the same point. Following the procedure by Biagi et al. (2007), the differences between the stroke positions within a flash are then computed from the position distances in the LLS data and are downscaled by $\sqrt{2}$. This scaling is necessary because both positions are subject to random errors (Biagi et al. 2007; Schulz et al. 2012). There is, however, the possibility that the channel geometry and/or the actual ground contact varied slightly from stroke to stroke and was not resolved by the video camera. Therefore, the differences determined by this method should be regarded as upper bounds of the actual position differences. A limited number of eight flashes has been observed with subsequent strokes following the same channel. However, not all of the networks observe all these flashes and/or strokes. We find an upper limit for the median LA of 6.1, 1.0, 0.6, 0.9, and 1.0 km for OP, TP, EUCLID, GLD360, and ATDnet, respectively. Figure 6 visualizes the spatial deviations for the strokes in the same channel w.r.t. the first stroke in that channel. For EUCLID, GLD360, and to a lesser extent ATDnet, the offsets follow a northwest–southeast direction, whereas TP tends to centralize the subsequent stroke positions around the first stroke. This behavior for the large-scale networks reflects the direction of the error ellipses being northwest–southeast directed. The LA by EUCLID over Belgium is about double of what is found from the Gaisberg tower observations (368 m) from a sample of 467 reported tower strikes and from video observations (330–440 m) based on 103 strokes in Austria (Schulz 2011). On the other hand, the LA of GLD360 is a few factors lower than the predicted 5–10 km, or when validated against NLDN (~10 km) and BrasilDAT (12.5 km) detections.
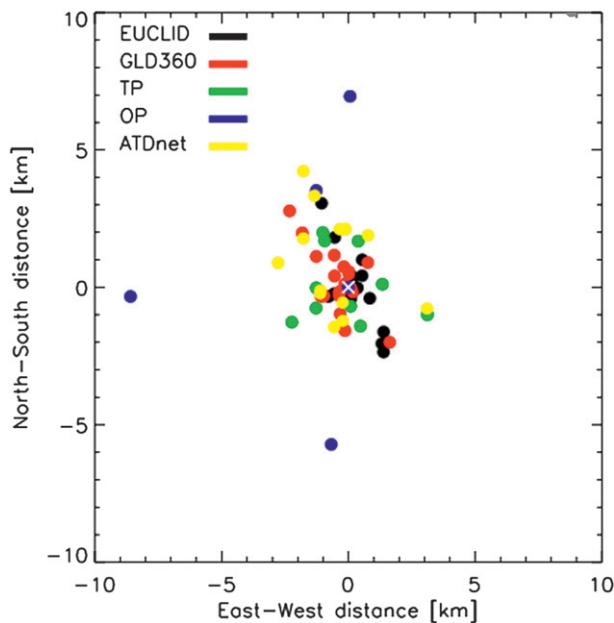
FIG. 6. Location offset for the subsequent strokes following the same channel as seen in the video images. The origin corresponds to the location of the first stroke in the channel.

TABLE 2. Distance between corresponding stroke positions.

	Median location difference (km)	No. of strokes*
OP vs TP	9.9	118
OP vs EUCLID	10.4	134
OP vs GLD360	10.9	108
OP vs ATDnet	10.7	96
TP vs EUCLID	1.0	126
TP vs GLD360	2.0	103
TP vs ATDnet	1.8	97
EUCLID vs GLD360	1.4	134
EUCLID vs ATDnet	1.9	113
GLD360 vs ATDnet	2.0	82

* The amount of strokes detected by the two networks.

Similar to Table 1, values for the 95% median confidence interval are reported in parentheses. We find for OP, TP, and ATDnet that the DE for a stroke with a new ground contact is larger than the DE for a stroke following a preexisting channel. This is explained by the fact that the median estimated peak current for NGCs is larger than the median for PECs. However, the opposite is found in the cases of EUCLID and GLD360, but it is probably related to the limited number of events. It is likely that a more extended dataset would bring the latter more in line with the expectations. Note that the medians for first strokes, as reported in Table 1, are larger than the medians in NGCs. In their turn, the medians in NGCs are larger than the medians in PECs.
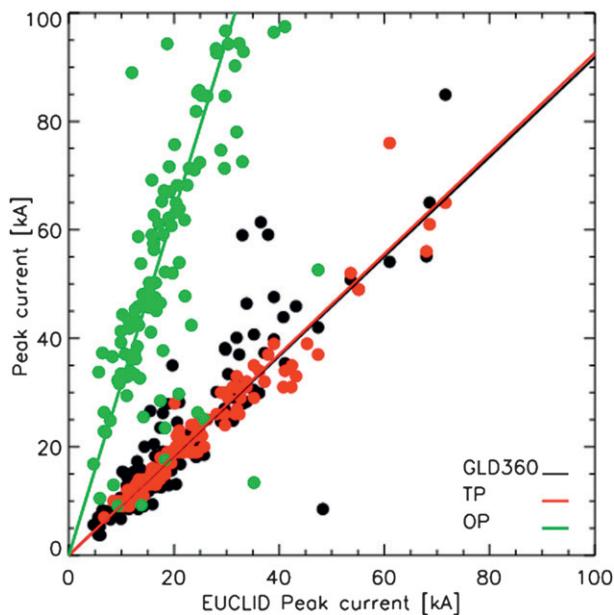
The same holds for ATDnet, for which the LA of 1 km is a few factors lower as projected (Keogh et al. 2006) or when compared to other networks (Schulz et al. 2000; Gaffard et al. 2008).

One can correlate the locations of the 210 individual strokes between two different networks. Results hereof are presented in Table 2. We find that when comparing a network against OP, the median location difference is 10 km or larger. This large location difference is attributed to the poor location accuracy of OP, as reported in Table 1, and is similar to the findings presented in Poelman (2011). The median location difference between overlapping strokes among the other networks ranges from 1 to 2 km, with the smallest spatial differences found between TP and EUCLID.

Estimated median stroke peak currents are compared as well. From Table 1, we find a good correlation between the peak currents measured by TP, EUCLID, and GLD360. However, OP seems to be off by a factor of ~3. This overestimation is likely due to a miscalibration of the SAFIR sensors. In line with the expectations, the reported median peak current for the first RS is higher than for the subsequent strokes. In Fig. 7, the EUCLID reported peak current versus the peak current of the other networks between corresponding strokes is plotted.

In Table 3 the DEs and estimated peak currents are listed solely for those subsequent strokes that follow a preexisting channel (PEC) or create a new ground contact (NGC), as captured by the high-speed camera.

FIG. 7. EUCLID reported peak current vs reported peak current by OP (green), TP (red), and GLD360 (black).

TABLE 3. DE and I_p for subsequent strokes that remained in a PEC and those that produced NGCs. In addition, 95% confidence intervals are reported in parentheses.

	No. of strokes on video	OP	TP	EUCLID	GLD360	ATDnet
Subsequent stroke DE (%) in PEC	34	56	38	76	65	47
Subsequent stroke DE (%) with NGC	15	60	47	53	53	60
Subsequent stroke I_p (kA) in PEC	34	−36.2 (−68, −32)	−15.0 (−24, −10)	−12.6 (−20, −10)	−10.7 (−20, −7)	—
Subsequent stroke I_p (kA) with NGC	15	−37.1 (−90, −20)	−20.0 (−28, −15)	−19.3 (−32, −10)	−18.0 (−29, −5)	—

This behavior is in agreement with other ground-truth campaigns (Fleenor et al. 2009; Biagi et al. 2007; Stall et al. 2009). In addition, it is worth mentioning that in our observations the majority (>80%) of the subsequent strokes that produce an NGC have a stroke number 2 or 3 within the flash.

Figure 8 plots the distribution of the amount of strokes detected within a single flash for each network, along with the distribution based on the camera and E-field observations. The observed percentage of single-stroke flashes is 21%. This value is comparable to what is found in other studies (Rakov and Uman 1990b; Kitagawa et al. 1962; Cooray and Jayaratne 1994); however, it seems to vary somewhat between 20% and 40% (Fleenor et al. 2009; Biagi et al. 2007). Thus, the majority are multistroke flashes, with a mean multiplicity of 2.8, 2.6, 3.1, 2.6, and 2.4 and a standard deviation of 1.7, 1.8, 1.6, 1.7, and 1.9 for OP, TP, EUCLID, GLD360, and ATDnet, respectively. Two flashes have even been observed by the field measurement system (with fields and E-fields) exhibiting 12 consecutive strokes. It is seen that all networks tend to overestimate the amount of single-stroke flashes compared to the observations and exhibit

a second peak around 2–3 strokes per flash, consistent with the observations. The overestimation of the amount of single-stroke flashes by the majority of the networks is related to the fact that first strokes tend to be, in general, more easily detected by an LLS because of its higher peak current compared to the subsequent strokes. As such, the amount of observed single-stroke flashes by an LLS is increased by a fraction of multistroke flashes from which only one stroke is detected.

Finally, Fig. 9 illustrates the stroke DE as a function of estimated peak current. First, for each stroke the mean of the peak currents estimated by TP, EUCLID, and GLD360 is calculated. This is allowed, since Fig. 7 shows a tight relation between the peak currents of these networks. From this, we retrieve a set of 192 strokes, of which we have an estimated peak current; that is, 18 strokes were not detected by TP, nor EUCLID and GLD360. Second, the DE is tested against this set for each network. In general, the DE is observed to rise with increasing peak current. However, this tendency is less pronounced for OP and ATDnet. For strokes with $|I_p| > 50$ kA, the DE is 100% for most of the networks.
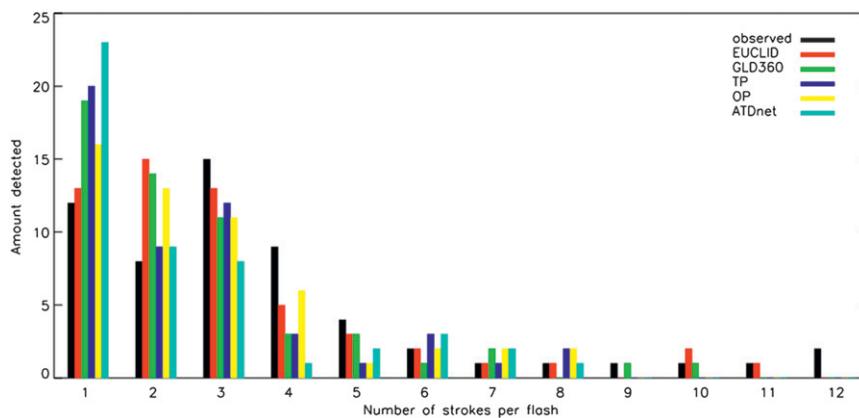

FIG. 8. Distribution of the observed multiplicity in negative flashes and as detected by the different networks.
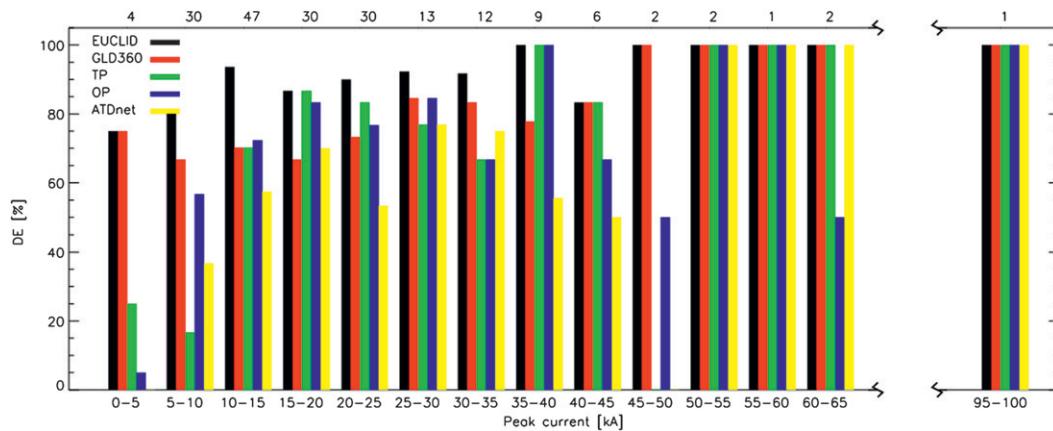
FIG. 9. Distribution of the DE for negative cloud-to-ground strokes as a function of peak current. The amount of strokes for each peak current interval is indicated on top of the figure.

5. Summary and discussion

E-field and high-speed camera observations were recorded during three thunderstorm days in Belgium. The data are used to determine the location accuracy, detection efficiency, and peak current estimates of some distinct lightning detection networks covering Belgium. Even though it is not the main focus of this paper, it is worth mentioning the observation of a continuing current exceeding 1 s following the last stroke in a two-stroke flash. Such a long continuing current is rarely observed in natural negative CG lightning.

At the level of flashes, all the networks perform well with a detection efficiency of over ~90%. Larger differences are found between the stroke detection efficiencies. EUCLID is the network with the highest overall detection efficiency.

The location accuracy of OP is rather poor. This is related to the location algorithm that uses the position of a time-correlated VHF signal as the CG striking point. As VHF emission can be transmitted from high above ground or in the cloud, this potentially leads to a large location difference compared to the true ground striking point. Based on a limited set of strokes that follow the same channel to ground, we retrieve median location accuracies for TP, GLD360, and ATDnet of about 1 km, a few hundred meters more than what is found for EUCLID. In addition, when correlating the positions of mutual observed strokes between two networks, it is found that TP and EUCLID locate its strokes closest to each other.

On the level of the estimated peak currents, it is noteworthy to stress that GLD360, being a global lightning detection network using a new technology, reports about the same median peak current as what is measured by EUCLID and TP. On the other hand, OP shows a large

deviation by a factor of 3 in the observed median peak current compared to the other lightning location systems.

After this ground-truth campaign, RMI found out with the help of Vaisala that the oscillators within the SAFIR sensors were not synchronized and each showed a time drift of about 4 µs. Since these time drifts were of the same order for all four SAFIR sensors, its influence on the location algorithm used within OP is minor. However, coupling the SAFIR sensors to LS-type sensors in TP has a significant impact on the stroke detection efficiency. We believe therefore that TP's performance, after tuning of the SAFIR sensors, improved with respect to the results presented in this paper. This needs to be tested with future ground-truth campaigns.

REFERENCES

Biagi, C. J., K. L. Cummins, K. E. Kehoe, and E. P. Krider, 2007: National Lightning Detection Network (NLDN) performance in southern Arizona, Texas, and Oklahoma in 2003–2004. *J. Geophys. Res.,* **112,** D05208, doi:10.1029/2006JD007341.

Brook, M., N. Kitagawa, and E. J. Workman, 1962: Quantitative study of strokes and continuing currents in lightning discharges to ground. *J. Geophys. Res.,* **67** (2), 649–659.

Cooray, V., and K. P. S. C. Jayaratne, 1994: Characteristics of lightning flashes observed in Sri Lanka in the tropics. *J. Geophys. Res.,* **99** (D10), 21 051–21 056.

Demetriades, N. W. S., M. J. Murphy, and J. A. Cramer, 2010: Validation of Vaisala's global lightning dataset (GLD360) over the continental United States. *Proc. 21st Int. Lightning Detection Conf.,* Orlando, FL, Vaisala, 6 pp. [Available online at http://www.vaisala.com/Vaisala%20Documents/Scientific%20papers/6.Demetriades,%20Murphy,%20Cramer.pdf.]

Diendorfer, G., 2010: LLS performance validation using lightning to towers. *Proc. 21st Int. Lightning Detection Conf.,* Orlando, FL, Vaisala, 15 pp. [Available online at http://www.vaisala.com/Vaisala%20Documents/Scientific%20papers/1.Keynote-Diendorfer.pdf.]

——, and W. Schulz, 2003: Ground flash density and lightning exposure of power transmission lines. *Proc. IEEE Power Tech Conf.,* Bologna, Italy, IEEE, doi:10.1109/PTC.2003.1304476.

Fleenor, S. A., C. J. Biagi, K. L. Cummins, E. P. Krider, and X.-M. Shao, 2009: Characteristics of cloud-to-ground lightning in warm-season thunderstorms in the central Great Plains. *Atmos. Res.,* **91,** 333–352.

Gaffard, C., and Coauthors, 2008: Observing lightning around the globe from the surface. *20th Int. Lightning and Detection Conf. (ILDC) and Second Int. Lightning Meteorology Conf. (ILMC),* Tucson, AZ, Vaisala, 12 pp. [Available online at http://www.vaisala.com/Vaisala%20Documents/Scientific%20papers/Observing_lightning_around_the_globe_from_the_surface.pdf.]

Idone, V. P., D. A. Davis, P. K. Moore, Y. Wang, R. W. Henderson, M. Ries, and P. F. Jamason, 1998a: Performance evaluation of the U.S. National Lightning Detection Network in eastern New York: 1. Detection efficiency. *J. Geophys. Res.,* **103** (D8), 9045–9055.

——, ——, ——, ——, ——, ——, and ——, 1998b: Performance evaluation of the U.S. National Lightning Detection Network in eastern New York: 2. Location accuracy. *J. Geophys. Res.,* **103** (D8), 9057–9069.

Jerauld, J., V. A. Rakov, M. A. Uman, K. J. Rambo, D. M. Jordan, K. L. Cummins, and J. A. Cramer, 2005: An evaluation of the performance characteristics of the U.S. National Lightning Detection Network in Florida using rocket-triggered lightning. *J. Geophys. Res.,* **110,** D19106, doi:10.1029/2005JD005924.

Keogh, S. J., E. Hibbett, J. Nash, and J. Eyre, 2006: Numerical weather prediction: The Met Office Arrival Time Difference (ATD) system for thunderstorms detection and lightning location. Met Office Forecasting Research Tech. Rep. 488, 22 pp.

Kitagawa, N., M. Brook, and E. J. Workman, 1962: Continuing currents in cloud-to-ground lightning discharges. *J. Geophys. Res.,* **67** (2), 637–647.

Lee, A. C. L., 1986: An experimental study of the remote location of lightning flashes using a VLF arrival time difference technique. *Quart. J. Roy. Meteor. Soc.,* **112,** 203–229.

——, 1989: Ground truth confirmation and theoretical limits of an experimental VLF arrival time difference lightning flash location system. *Quart. J. Roy. Meteor. Soc.,* **115,** 1147–1166.

Naccarato, K. P., O. Pinto Jr., S. A. M. Garcia, M. Murphy, N. Demetriades, and J. Cramer, 2010. Validation of the new GLD360 dataset in Brazil: First results. *Proc. 21st Int. Lightning Detection Conf.,* Orlando, FL, Vaisala, 6 pp. [Available online at http://www.vaisala.com/Vaisala%20Documents/Scientific%20papers/7.Naccarato,%20Pinto,%20Garcia.pdf.]

Nag, A., and Coauthors, 2011: Evaluation of U.S. National Lightning Detection Network performance characteristics using

rocket-triggered lightning data acquired in 2004–2009. *J. Geophys. Res.,* **116,** D02123, doi:10.1029/2010JD014929.

Poelman, D. R., 2011: Present status and preliminary results of the Belgian lightning detection network. *Proc. Sixth European Conf. on Severe Storms,* Palma De Mallorca, Balearic Islands, Spain, ECSS, 3 pp. [Available online at http://www.essl.org/ECSS/2011/programme/abstracts/92.pdf.]

Rakov, V. A., and M. A. Uman, 1990a: Long continuing current in negative lightning ground flashes. *J. Geophys. Res.,* **95** (D5), 5455–5470.

——, and ——, 1990b: Some properties of negative cloud-to-ground lightning. *Proc. 20th Int. Conf. on Lightning Protection,* Interlaken, Switzerland, ICLP, Paper 6.4.

——, and ——, 1991: Long continuing currents in negative cloud-to-ground lightning flashes: Occurrence statistics and hypothetical mechanism. *Izv. Akad. Nauk SSSR, Fiz. Atmos. Okeana,* **27,** 376–330.

Saba, M. M. F., O. Pinto Jr., and M. G. Ballarotti, 2006: Relation between lightning return stroke peak current and following continuing current. *Geophys. Res. Lett.,* **33,** L23807, doi:10.1029/2006GL027455.

Said, R. K., U. S. Inan, and K. L. Cummins, 2010: Long-range lightning geolocation using a VLF radio atmospheric waveform bank. *J. Geophys. Res.,* **115,** D23108, doi:10.1029/2010JD013863.

——, M. J. Murphy, N. W. S. Demetriades, K. L. Cummins, and U. S. Inan, 2011: Methodology and performance estimates of the GLD360 lightning detection network. *Proc. 14th Int. Conf. on Atmospheric Electricity,* Rio de Janeiro, Brazil, ICAE, 243. [Available online at http://www.icae2011.net.br/upload/resumos.pdf.]

Schulz, W., 2011: Performance evaluations of the European Lightning Location System EUCLID. *Proc. Sixth European Conf. on Severe Storms,* Palma de Mallorca, Balearic Islands, Spain, European Severe Storms Laboratory, 9.1. [Available online at http://www.essl.org/ECSS/2011/programme/presentations/9_1.pdf.]

——, and M. Saba, 2009: First results of correlated lightning video images and electric field measurements in Austria. *Proc. 10th Int. Symp. on Lightning Protection,* Curitiba, Brazil, SIPDA, 3 pp.

——, G. Diendorfer, M. Dorninger, and N. Daly, 2000: Comparison of lightning data collected by location systems of different technology. *Proc. 16th Int. Lightning Detection Conf. (ILDC),* Tucson, AZ, Vaisala, 6 pp.

——, B. Lackenbauer, H. Pichler, and G. Diendorfer, 2005: LLS data and correlated continuous field measurements. *Proc. Eighth Int. Symp. on Lightning Protection,* São Paulo, Brazil, SIPDA, 4 pp.

——, H. Pichler, and G. Diendorfer, 2010: Evaluation of 45 negative flashes based on E-field measurements, video data and lightning location data in Austria. *Proc. 30th Int. Conf. on Lightning Protection,* Cagliari, Italy, Power and Energy Society, 1011-1–1014. [Available online at http://www.aldis.at/pdf/12_135_ICLP_SCH_PI_DIN.pdf.]

——, C. Vergeiner, H. Pichler, G. Diendorfer, and K. Cummins, 2012: Location accuracy evaluation of the Austrian Lightning Location System ALDIS. *Proc. 22nd Int. Lightning Detection Conf.,* Broomfield, CO, Vaisala, 5 pp.

Stall, C. A., K. L. Cummins, E. P. Krider, and J. A. Cramer, 2009: Detecting multiple ground contacts in cloud-to-ground lightning flashes. *J. Atmos. Oceanic Technol.,* **26,** 2392–2402.